CD19-targeting CAR T cells potently redirected to kill solid tumor cells

Christine Ambrose[1], Lihe Su[1], Lan Wu[1], Fay Dufort[1], Thomas Sanford[1], Alyssa Birt[1], Benjamin Hackel[2], Andreas Hombach[3], Hinrich Abken[3,§], Roy R Lobb[1] and Paul D. Rennert[1*]. 1: Aleta Biotherapeutics, 27 Strathmore Rd, Natick, MA 01760 USA. 2: University of Minnesota, 421 Washington Avenue SE, Minneapolis, MN 55455. 3: University of Cologne, Albertus-Magnus-Platz, Köln, Germany.

* Correspondence should be addressed to P.D.R (paul.rennert@aletabio.com)

§ current address: Regensburg University, Universitätsstraße 31, 93053 Regensburg, Germany.

CAR-CD19 T cells used to target solid tumors

Abstract

Successful CAR T cell therapy for the treatment of solid tumors requires exemplary CAR T cell expansion, persistence and fitness, and the ability to target tumor antigens safely. Here we address this constellation of critical attributes for successful cellular therapy by using integrated technologies that simplify development and derisk clinical translation. We have developed a CAR-CD19 T cell that secretes a CD19-anti-Her2 bridging protein. This cell therapy strategy exploits the ability of CD19-targeting CAR T cells to interact with CD19 on normal B cells to drive expansion, persistence and fitness. The secreted bridging protein potently binds to Her2-positive tumor cells, mediating CAR-CD19 T cell cytotoxicity *in vitro* and *in vivo*. Because of its short half-life, the secreted bridging protein will selectively accumulate at the site of highest antigen expression, ie. at the tumor. Bridging proteins that bind to multiple different tumor antigens have been created. Therefore, antigen-bridging CAR-CD19 T cells incorporate critical attributes for successful solid tumor cell therapy. This platform can be exploited to attack any cancer.

Introduction

The treatment of relapsed or refractory Acute Lymphocytic Leukemia (ALL) and Non-Hodgkin Lymphoma (NHL) with chimeric antigen receptor (CAR) T-cells that target CD19 (CAR-CD19 T cells) has led to FDA and EMA approvals of the adoptive cell therapies tisagenlecleucel and axicabtagene ciloleucel [1,2]. CAR-CD19 T cells have thus paved the way for the development of cellular therapeutics as 'living drugs', and have driven our understanding of CAR T cell regulatory, CMC and commercialization issues [3]. Furthermore, CAR-CD19 T cells are routinely used to evaluate all aspects of CAR T cell function, including optimization of signaling domains and hinge regions [4], development of dual CARs [5,6], expression of cytokines, antibodies, and other mediators [7,8], evaluation of toxicities [9,10], and of switch technologies [11,12]. CAR-CD19 T cells also provide a simple and universal solution to the issue of CAR T cell persistence. Robust *in vivo* expansion followed by prolonged CAR-T cell persistence is critical for their efficacy in the treatment of hematologic malignancies [13,14]. Since CD19-positive normal B cells are constantly produced by the bone marrow in response to B cell aplasia, CAR-CD19 T cells uniquely access a non-tumor dependent and self-renewing source of activating antigen. This is true even in patients who have undergone lymphodepleting chemotherapy as the bone marrow can recover and start producing B cells in as little as 28 days [15,16]. In contrast, other CAR T cells, particularly those targeting solid tumor antigens, have largely shown poor persistence to date [17]. In short, CAR-CD19 T cells have properties which make them uniquely suited to CAR T cell therapy, come with a broad and expanding set of pre-clinical knowledge and possess an unmatched development history.

To capitalize on this deep knowledge base, we have chosen to use CAR-CD19 T cells as a unique platform solution that will allow us to target and kill any tumor. We recently described

the development of bridging proteins which contain the extracellular domain (ECD) of CD19 linked to an antigen binding domain, eg. an antibody fragment, that binds to a tumor-expressed antigen [18]. The wild-type CD19 ECD was difficult to express, therefore we developed stable CD19 ECD mutants that can be linked N- or C-terminally to any protein, generating modular CD19 bridging proteins with enhanced secretion and a predicted lack of immunogenicity [18]. These rationally designed CD19 bridging proteins are capable of binding to any tumor antigen, thereby coating CD19-negative tumor cells with CD19. CD19-coated tumor cells representing diverse indications were thereby made susceptible to potent CAR-CD19 T cell-mediated cytotoxicity [18]. Of note, the CAR-CD19 domain on the T cell remains the same regardless of the antigens targeted by the bridging protein, and this minimizes complexity in CAR T cell manufacturing across our diverse programs. This technology therefore has the potential to broaden the reach of CAR-CD19 T cells beyond B cell malignancies to any tumor without the need to build many different CAR and combination CAR constructs. Given the emerging knowledge regarding the need for multi-antigen targeting in order to ensure durable responses to CAR-T therapy the need for such a simple, pragmatic and modular technology is evident.

Here we describe the use of CAR-CD19 T cells that secrete CD19 bridging proteins as a highly effective therapeutic approach to targeting hematologic cancers and solid tumors. CD19 bridging proteins are simple and modular solutions to multi-antigen targeting, antigen selectivity, and optimization of potency and safety. This technology retains the inherent advantages of CAR-CD19 T cells and leverages the development and manufacturing knowledge accumulated to date.

Results

CD19-anti-Her2 bridging proteins are stable monomers with potent binding affinities

We have shown that wildtype and stabilized mutant forms of the CD19 ECD can be fused to a variety of scFvs, VHHs, and scaffold proteins such as Fibronectin Type III (Fn3) domains, with the retention of binding function, CAR-CD19 recognition and cytotoxicity [18,19]. These CD19-containing fusion proteins bind to both CAR-CD19 T cells and to the targeted tumor antigens, and are referred to as bridging proteins. Here we show that bridging proteins can be secreted by CAR-CD19 T cells transduced with a lentiviral vector construct that encodes both a cell surface CAR-CD19 sequence and a bridging protein sequence.

Prior to creating specific lentiviral expression constructs, we characterized the purified bridging proteins in detail to assess their biophysical properties as exemplified here with a CD19-anti-Her2 scFv bridging protein that contains the wildtype CD19 ECD fused to an anti-Her2 scFv derived from trastuzumab (construct #42, Table 1). The bridging protein was expressed in construct #42-transfected 293T cell supernatants and analyzed using PAGE and Western blot analyses. Under non-reducing PAGE conditions, the majority of the secreted bridging protein was monomeric, with some larger molecular weight (MW) bands observed (Supplemental Fig. S1a). The monomeric form with the expected MW was separated by gel filtration from the larger MW species and analyzed by PAGE under reducing and non-reducing conditions (Supplemental Fig. S1b). The control proteins wildtype CD19 ECD (#28) and CD22 ECD-anti-Her2 scFv (#117) (see Table 1) were also analyzed after gel filtration (Supplemental Fig. S1b). The gel filtration fractions representing monomer and higher MW species were tested for binding in an ELISA assay using anti-CD19 antibody FMC63 as the capture reagent and Her2-Fc as the detection reagent. In this ELISA format the monomeric form bound with an EC_{50}

of 2.5 nM, but the aggregated form bound poorly and the control protiens did not bind (Supplemental Fig. S2a, Table 2 and data not shown). These results are similar to our previously reported ELISA results using anti-CD19 antibody FMC63 capture and anti-His antibody detection (EC_{50} = 2.7 nM) [18]. When the ELISA format was reversed (Her2-Fc capture, FMC63 detection) the purified CD19-anti-Her2 bridging protein (#42) bound to the anti-CD19 antibody FMC63 with an apparent EC_{50} of 0.4 nM (Supplemental Fig. S2b).

Table 1. List of construct numbers used in the text, presented in the numerical order with a description of the encoded sequences in column 2 and the format in which the expressed sequence is utilized in column 3. CD19 ECD-A and CD19 ECD-B are described in the methods section. The long dashes indicate a linker sequence. P2A refers to a cleavage sequence. BP refers to a bridging protein.

Construct #	Description	Modality
28	CD19 ECD-A	Purified protein
42	CD19 ECD-A – anti-Her2	Purified BP
117	CD22 ECD – anti-Her2	Purified BP
142	Sequence of 254 – P2A – sequence of 42	CAR-CD19 + BP
254	CAR sequence targeting CD19	CAR-CD19
311	Stabilized CD19 ECD-B	Purified BP
340	Stabilized CD19 ECD-A – anti-Her2	Purified BP
374	Sequence of 254 – P2A – sequence of 340	CAR-CD19 + stabilized BP
390	CAR sequence targeting Her2	CAR-Her2
416	Stabilized CD19 ECD-B – anti-EGFR	Purified BP
460	Anti-Her2 – stabilized CD19 ECD-A – anti-EGFR	Purified BP

Bridging protein #340 is identical to #42, except that a stabilized form of the CD19 ECD was used, as described presiously [18]. The purified monomeric forms of proteins #42 and #340 were stable when incubated for 3 days at 37°C, with minimal aggregation or clipping observed (Western blot analyses, data not shown). The #42 bridging purified protein preparation was shown to contain some dimer species, which were not present in the #340 purified bridging protein preparation (data not shown). When the two bridging proteins, #42 and #340, were tested for binding to anti-CD19 antibody FMC63 in an ELISA format (FMC63 capture, Her2-Fc detection), the CD19 stabilized protein #340 bound with higher affinity (EC_{50} = 0.08, Table 2). A difference in binding affinity was less apparent when the ELISA assay format was reversed (Her2-Fc capture, FMC63 detection) (Table 2).

Table 2. Summary of bridging protein binding and cytotoxicity data. Top: EC_{50} binding data for bridging proteins and control proteins as determined in ELISA assays. The capture reagents, detection reagents and protein construct numbers are indicated. Middle: EC_{50} binding data for bridging proteins and control proteins as determined in flow cytometric assays. The cells used are indicated. Flow cytometry reagents used to detect cell-bound proteins are indicated parenthetically. Bottom: bridging protein-mediated CAR-CD19 cytotoxicity against Her2-positive cell lines. CAR-CD19 T cells from donor 54 (47% CAR-positive) and donor 69 (54% CAR positive) were used at an E:T ratio of 10:1. IC_{50} values were derived from a titration of the bridging protein concentration in the assays. A dash (-) indicates no binding or activity above background. ND indicates 'not done'.

Bridging protein binding affinity in ELISA assays (EC_{50}, nM)					
CAPTURE	**DETECTION**	**#42**	**#340**	**#28**	**#117**
FMC63	Her2-Fc	2.5	ND	-	-
FMC63	Her2	0.3	0.08	-	-
Her2-Fc	FMC63	0.4	0.16	-	-
Bridging protein binding affinity in flow cytometric assays (EC_{50}, nM)					
Cells	CAR-CD19 T	0.48 (anti-His)	0.2 (anti-His)	-	-

	cells				
	untransduced T cells	-	-	-	ND
	SKOV3	1.7 (anti-His) 1.1 (FMC63)	2.7 (anti-His) 1.5 (FMC63)	-	0.7 (anti-His) 1.5 (anti-CD22)
	BT474	0.3 (FMC63)	0.2 (FMC63)	-	0.5 (anti-His)
Bridging protein mediated cytotoxicity (IC_{50}, pM)					
Donor	**Target cells**	**#42**	**#340**	**#28**	**#117**
54	SKOV3	3	2	-	-
69	BT474	13.5	7.1	-	-

Flow cytometry was used to characterize the binding of the bridging proteins to cells. Donor human T cells were transduced with lentiviral particles that express the scFv derived from the anti-CD19 antibody FMC63 (CAR-CD19, encoded by construct #254, Supplemental Fig. 3a). The binding of the CD19-anti-Her2 bridging protein (#42) to CAR-CD19 T cells was analyzed in a flow cytometry dose response assay, yielding an EC_{50} of 0.48 nM (Supplemental Fig. 3b). Bridging protein #340 bound to CAR-CD19 T cells with a slightly higher affinity of 0.2 nM; this was statistically significant (Supplemental Fig. 3b). Neither molecule bound to un-transduced T cells (UTD) from the same donor (Supplemental Fig. 3b). SKOV3 ovarian carcinoma cells express Her2 (Supplemental Fig. 3c). Bridging protein #42 bound SKOV3 cells with an EC_{50} of 1.7 nM and the CD19 stabilized bridging proteins #311 and #340 bound SKOV3 cells with an EC_{50} of 0.2 nM and 3.2 nM respectively (Supplemental Fig. 3d). Two forms of the CD19 ECD with slightly different C-terminal sequences were evaluated (see Materials and

Methods). The bridging proteins bound to Her2-positive cells with very similar affinity whether the CD19 domain was wildtype ECD-A (#42), stabilized ECD-A (#340) or stabilized ECD-B (#311). In additional flow cytometry assays (n = 2 to 6 repeats) using Her2-positive SKOV3 and BT474 cells, purified #42 bound with an EC_{50} ranging from 0.3 - 1.7 nM, and purified #340 bound with an EC_{50} ranging from 0.2 – 2.7 nM (Table 2). The control bridging protein #117 (CD22-anti-Her2 scFv) bound to Her2-positive cells but not to CAR-CD19 T cells and the control protein CD19-ECD (#28) did not bind (Table 2). These data showed that both halves of the CD19-anti-Her2 bridging proteins were fully functional, binding to the CAR expressing the anti-CD19 FMC63 scFv and to the Her2 antigen on the SKOV3 cell surface. The protein binding data for ELISA and flow cytometric assays are summarized in Table 2.

CD19-bridging proteins do not compromise CAR-CD19 function

Aberrant signaling can drive CAR T cells into a dysfunctional state [20]. Therefore we assessed the impact of the bridging proteins #42 and #340 on CAR-CD19 T cell cytotoxicity against the target cell lines Nalm6 (CD19-positive) and SKOV3 (Her2-positive). CAR-CD19 T cells were generated using lentiviral particles encoding an anti-CD19 CAR domain (#254, Table 1). Cytotoxicity against Nalm6 cells requires that the CAR-CD19 is available to directly kill the cells. For the SKOV3 cells, cytotoxicity will occur when the CD19-anti-Her2 bridging protein binds to both the CAR-CD19 T cells and the target tumor cells, thereby forming a cytotoxic synapse. The components of the cytotoxicity assay were added in three ways: a) CAR-CD19 T cells, bridging proteins and target cells where added together at same time, b) CAR-CD19 T cells were added to a premixture of bridging proteins and target tumor cells, which had been pre-incubated at 37°C for 10 minutes, or c) the CAR-CD19 T cells were premixed with bridging

proteins and pre-incubated at 37°C for 10 minutes, and then added to target tumor cells. In all instances the bridging proteins were added at 1 μg/ml for each protein, a concentration shown to be saturating for binding to CAR-CD19 T cells (see Supplemental Fig. 3d). There was no difference in the degree of cytotoxicity observed among the three different conditions on either Nalm6 cells (Fig. 1a) or SKOV3 cells (Fig. 1b). These experiments demonstrated that pre-binding of the CD19-anti-Her2 bridging protein does not negatively impact the ability of the CAR-CD19 T cells to directly or indirectly kill the target cells.

Figure 1. CAR-CD19 and bridging proteins have potent cytotoxic activity *in vitro*. A,B) Bridging proteins, CAR-CD19 T cells and target tumor cells were added simultaneously (red bars) or bridging proteins and tumor cells were preincubated then added to CAR-T cells (light blue bars) or bridging proteins and CAR-T cells were preincubated then added to tumor cells (black bars). Controls were CAR T cells directed to the target antigen (Cells, diagonal bars) or target cells alone in culture (Cells, zero cytotoxicity). Nalm6 (A) and SKOV3 (B) cytotoxicity is shown using bridging proteins #42 and #340. C) Donor CAR-254 T cells were tested for cytotoxicity against Nalm6 cells at different E:T ratios compared to donor-matched UTD cells (10:1, blue; 3:1, teal; 1:1 light blue). D,E) Dose response cytotoxicity curves using a fixed E:T ratio of CAR-254 and target cells and varying the concentration of the bridging proteins #42 and #340 or the control protein #28. Target cell lines SKOV3 (D) and BT474 (E) are shown.

To address the potency of direct cytotoxicity via CD19 binding, CAR-CD19 T cell cytotoxicity was determined at different effector:target (E:T) ratios using Nalm6 cells and CAR-254. Cytotoxicity was routinely observed down to the lowest E:T ratio tested, although there was some variation in the extent of cytotoxicity depending on the specific normal human donor T cells used in the assay; data obtained using donor 69 are shown (Fig. 1c). Next, CAR-CD19 T cell cytotoxicity curves were derived for killing SKOV3 cells in the presence of the #42 and #340 bridging proteins. The bridging proteins mediated very potent cytotoxicity with IC_{50} values of 2-3 pM (Fig. 1d). Similar results were obtained using a second Her2-positive target cell line, BT474, where derived the IC_{50}s were 13.5 pM and 7.1 pM for the #42 and #340 bridging

proteins, respectively (Fig. 1e, Table 2). These data demonstrate cytotoxicity IC_{50} values in the low pM range.

A dual-antigen-directed bridging protein potently targets Her2 and EGFR

Having successfully engineered CD19-anti-Her2 scFv bridging proteins we added a second antigen-targeting domain. An anti-EGFR scFv was encoded in frame with the sequence of construct #42 to create construct #460 (Table 1). Construct #460 was used to transfect 293T cells and the secreted dual-antigen targeting bridging protein was purified. The binding characteristics of this bridging protein for the target antigens Her2 and EGFR were established by flow cytometric assays as described above, with the addition of EGFR-positive cell binding data (Table 3). The dose responsive binding of the bridging protein to Her2-positive and EGFR-positive cells (#460) produced EC_{50} values of 2.5 nM and 0.6 nM, respectively. The potency of the multi-antigen bridging protein in mediating CAR-CD19 T cell cytotoxicity against Her2-positive, EGFR-positive and dual-antigen-positive cell lines was determined and IC_{50} values were calculated (Table 3). Dual antigen bridging protein-mediated cytotoxicity was highly effective against single antigen-positive cells, whether Her2-positive or EGFR-positive, with IC_{50} values ranging from 5 pM - 19 pM (Table 3). Notably, bridging protein-mediated cytotoxicity was more potent against multi-antigen positive cell lines, with IC_{50} values of 1.4 pM (SKOV3) and 2.6 pM (A431) (Table 3). The single antigen bridging protein controls (#311 and #416, Table 1) were a log or more less potent on the dual antigen expressing cell lines SKOV3 and A431. These results demonstrate effective multi-antigen targeting by a single bridging protein.

Table 3. Activity of dual antigen binding bridging protein #460. Top: Binding of single antigen and dual antigen bridging proteins to single and dual-antigen positive cell lines. Binding was detected with anti-CD19 antibody FMC63 staining and the EC_{50} values were derived from dose response flow cytometric analyses. A dash indicates that there was no detectable binding. Bottom: Bridging protein-mediated CAR-CD19 cytotoxicity against Her2-positive cell lines. CAR-CD19 T cells were used at an E:T ratio of 10:1. IC_{50} values were derived from a titration of the bridging protein concentration in the assays. ND: not done.

Bridging protein binding affinity in flow cytometry assays (EC_{50}, nM)				
cell line	**expressed antigens**	**#460 (dual binding)**	**#311 (anti-Her2)**	**#416 (anti-EGFR)**
BT474	Her2 only	2.5	3.1	-
K562-EGFR	EGFR only	0.6	-	0.52
SKOV3	Her2-high, EGFR-low	0.44	1.85	0.37
A431	Her2-low, EGFR-high	0.15	-	0.1
Bridging protein mediated cytotoxicity by CAR-CD19 T cells (IC_{50}, pM)				
BT474	Her2 only	5	20.4	ND
K562-EGFR	EGFR only	19.1	ND	20.9
SKOV3	Her2-high, EGFR-low	1.4	11.7	13
A431	Her2-low, EGFR-high	2.6	1700	44.8

CD19-bridging proteins do not bind the CD19-cis ligands CD21 and CD81

CD19 binds CD21 in cis and reportedly binds tetraspanins such as CD81 [21,22]. We used a panel of cell lines expressing CD20 (Raji), CD21 (Raji), CD81 (Raji, SKOV3, K562), and Her2

(SKOV3), or none of these antigens (U937), to evaluate potential trans-binding of the CD19 bridging proteins. Bindng of CD19-anti-Her2 bridging proteins (#42 and #340) to all four cell lines was evaluated by flow cytometry using an anti-His-tag antibody and the anti-CD19 antibody FMC63. As expected, the CD19 anti-Her2 bridging proteins bound SKOV3 cells via the anti-Her2 scFv. The bridging proteins did not bind to Raji cells (Her2-negative, CD21-positive, CD81-positive) as detected by anti-His-tag antibody staining (Supplemental Table S1). Detection of bridging protein with the anti-CD19 antibody FMC63 is possible for those cell lines which are CD19-negative: binding was observed with SKOV3 cells (Her2-positive, CD81-positive) but not with K562 cells (Her2-negative, CD81-positive) or U937 cells (negative for CD21, CD81 and Her2) (Supplemental Table S1). We previously showed that CAR-CD19 T cells do not kill SKOV3 cells via CD81 binding in the presence of the CD19 ECD control protein (#28), but only in the presence of the CD19-anti-Her2 bridging protein [18]. These results show that the CD19 ECD, whether wild-type or stabilized, cannot interact with either CD21 or CD81.

CD19-anti-Her2 bridging proteins are secreted by CAR-CD19 T cells

To generate CAR-CD19 cells that secrete bridging proteins we cloned the sequence of bridging proteins #42 or #340 into a lentiviral vector downstream of a CAR-CD19 sequence (#254) and a P2A site to create CAR-142 and CAR-374, respectively (Table 1). Viral particles were produced with a transducing titer of 1.8×10^9 TU/ml for CAR-142 and 2.5×10^9 TU/ml for CAR-374. T cells isolated from human donors were transduced with the lentiviral particles and analyzed for expression of the CAR-CD19 domain by flow cytometry using an anti-Flag tag antibody for detection. Using 6 different donors, we determined that expression of the CAR-CD19 domain on the transduced primary T cells averaged 40% for CAR-142 and averaged 43% for CAR-374.

Bridging protein secretion was measured by ELISA (FMC63 capture and anti-His detection). The secretion of the bridging protein in activated T cell culture supernatants averaged 11.4 ng/ml for CAR-142 (n=4 donors, range 6-18 ng/ml) and 40.2 ng/ml for CAR-374 (n=7 donors, range 10-81 ng/ml) in activated CAR T cell culture supernatants.

We detected minimal bridging protein bound on the cell surface of the transduced T cells by flow cytometry for the two CAR-CD19 T cell secreted bridging proteins; in general increased staining of the bridging protein on the CAR-CD19 T cell surface correlated with higher levels of cell surface CAR-CD19 expression and with higher levels of secreted bridging protein measured in the cell culture supernatant (data not shown).

CAR-CD19 T cells that secrete CD19-anti-Her2 bridging proteins have potent activity *in vitro*

CAR-CD19 T cells secreting CD19-anti-Her2 bridging proteins (CAR-142 and CAR-374) were generated using normal human T cells (donor 45). The lentiviral transductions produced 42% CAR-positive T cells for both viral particle preparations, and the T cell pool was 50% CD8-positive (data not shown). CAR-142 and CAR-374 T cells were tested in cytotoxicity assays using either CD19-positive Nalm6 cells or Her2-positive SKOV3 cells at different E:T ratios; untransduced donor T cells were used as a negative control. CD19-positive Nalm6 cells were potently killed by CAR-142 or CAR-374 T cells, showing that the bridging protein did not interfere with CD19 recognition by the CAR-CD19 domain (Fig. 2). Her2-positive SKOV3 cells were also potently killed by both CAR-142 and CAR-374 T cells, demonstrating that the secretion of the bridging protein was sufficient to retarget the CAR-CD19 domain to SKOV3 cells. Potent cytotoxicity was seen down to an E:T ratio of 1:1 (Fig. 2). In this assay, the activity of CAR-142 and CAR-374 T cells was indistinguishable even though the amount of measured

bridging protein from activated CAR T cell cultures was ~5-fold higher for CAR-374 than CAR-142 (data not shown). This difference reflects the higher secretion level obtained using the stabilized CD19 ECD-anti-Her2 bridging protein (in CAR-374) versus the wildtype CD19 ECD-anti-Her2 bridging protein (in CAR-142).

Figure 2. Her2-bridging CAR-CD19 T cells are cytotoxic against both CD19-positive and Her2-positive cells *in vitro*. CAR T cells (CAR-142 or CAR-374) were added at different E:T ratios to Nalm6 cells (A) or SKOV3 cells (B) and cytotoxicity was measured. E:T ratios used were 10:1 (red bars), 3:1 (light blue bars) and 1:1 (black bars). The donor matched UTD cells are also shown at each E:T ratio.

These results show that CAR-CD19 T cells secreting a CD19-bridging protein that targets Her2 can efficiently kill Her2-positive target cells. This is the first demonstration of cytotoxic elimination of CD19-negative tumor cells by retargeted CAR-CD19 T cells. To generalize the approach, we generated a panel of CD19-bridging proteins and incorporated them into CAR-CD19-containing lentiviral vector constructs. In each case the transduced CAR-CD19 T cells (CAR-254) secreted ng/ml levels of bridging protein in the T cell activation assay (Supplemental Table S2). The secreted bridging proteins retargeted the CAR-CD19 T cells and mediated potent cytotoxicity, eg. to a CD20-positive cell line using a wildtype or stabilized CD19-anti-CD20 scFv bridging protein, to a BCMA expressing myeloma cell line, H929, using a wildtype CD19-anti-BCMA scFv bridging protein and to the AML cell line U937 using wildtype CD19-anti-Clec12a scFv bridging protein or using a stabilized CD19-anti-Clec12a VHH bridging protein (data not shown).

Successful repetitive CAR T cell stimulation *in vitro* predicts potent CAR T cell activity *in vivo* [23], as repetitive stimulation models the waves of functional activity and cell proliferation

needed for serial cytotoxicity. In the first set of experiments we exposed CAR-142 T cells to SKOV3 cells for 2 days, then removed the cells, rested them for 5 days and then re-exposed them to SKOV3 cells for 2 days. This was repeated for a total of 3 re-stimulations. CAR T cell cytotoxic activity against SKOV3 tumor cells was monitored during the course of the study. CAR-142 T cells were successfully re-stimulated through four rounds of exposure to SKOV3 cells (data not shown). However, CAR T cell numbers recovered after the third and fourth round were limited, suggesting that the proliferative potential of the T cell population had waned. In contrast, robust T cell numbers were generated from CAR-142 cells that were exposed to B cell lines for 2 days, then rested, then repeatedly restimulated using the same protocol (data not shown).

One variable that complicates analysis of the re-stimulation assay results is the differential proliferative capacity of target cells during the course of the *in vitro* cell culture based cytotoxicity assay. Suspension-cultured B cell lines undergo rapid proliferation whereas attachment-cultured SKOV3 cells divide much more slowly and become contact-inhibited once confluent. In order to control for potential differential target cell proliferation in the assay we used mitomycin-c treatment to stop cell proliferation. Mitomycin-c is a double-stranded DNA alkylating agent that covalently crosslinks DNA, inhibiting DNA synthesis and cell proliferation. The cells treated were CD19-positive Raji lymphoma cells and Her2-positive SKOV3 ovarian carcinoma cells and the doses used were sublethal for at least 48 hours [24,25].

Target tumor cells were treated with mitomycin-c, washed extensively, then cultured with CAR T cells for 48 hours. The CAR T cells were then rested for 48 hours before being restimulated with a new preparation of mitomycin-c treated target cells. The process of stimulation, rest and restimulation was repeated through 4 cycles, through day 15. The data are

expressed as fold-increase over day 0, normalized to 100 to account for variation across different experiments and donors (Fig. 3a). Representative results are given in the text. In the first experiments CAR-374 T cells were stimulated repeatedly with either Raji cells or with SKOV3 cells. CAR-374 T cells proliferated robustly in response to Raji cell restimulation through 4 rounds as did CAR-CD19 T cells (CAR-374: 24 fold; CAR-254: 56 fold). In contrast, CAR-374 T cells did not increase dramatically above day 0 cell numbers when restimulated with SKOV3 cells, nor did CAR-Her2 T cells (CAR-374: 2-fold; CAR-390: 1.3-fold). The results are shown normalized to maximum fold increase in each experiment (Fig. 3a). The differences in increase in response to Raji cell restimulation versus CAR T cells alone or to SKOV3 restimulation were highly significant at days 8, 12 and 15 ($p < 0.001$, t-test for two independent samples for each comparison, using the raw data (n=3)). The cells restimulated with SKOV3 only had not died, and they retained some cytotoxic activity through round 3 of stimulation (see below).

Figure 3. Her2-bridging CAR-CD19 and control CAR T cell proliferation in response to Raji cell stimulation or SKOV3 cell stimulation in the restimulation assay. Data are normalized to 100 across different studies and donors. A) CAR T cell proliferation in response to Raji cell restimulation (B>B), Raji cell stimulation followed by SKOV3 stimulation (B>S), SKOV3 restimulation (S>S), or SKOV3 stimulation followed by Raji stimulation (S>B). Cell count days are shown below the x-axis. An * indicates a statistically significant difference from the culture o CAR T cells alone. CAR-374 = Her2-bridging CAR-CD19; CAR-254 = CAR-CD19; and CAR-390 = CAR-Her2. B) Cytotoxicity of restimulated CAR-374 T cells against JeKo-1 or SKOV3 cells after 1 round or 3 rounds of stimulation. Cell stimulations are shown on the x-axis following the nomenclature from (A). C) Cytotoxicity of restimulated CAR-254 T cells (left) and CAR-390 T cell (right) against Nalm6 or SKOV3 cells after 1 round or 3 rounds of stimulation. Cell stimulations are shown on the x-axis following the nomenclature from (A).

To investigate if exposure of the CAR-374 T cells to the mitomycin-c-treated B cell line was having a beneficial effect on the activity of the T cells we next alternated exposure to B cells

or to SKOV3 solid tumor cells. CAR-374 T cells exposed to Raji cells for 1 or 2 cycles prior to being exposed to SKOV3 cells retained the ability to proliferate through 4 rounds of stimulation with activity similar to that of 4 rounds of exposure to Raji cells (Fig. 3a). Two prior rounds of exposure to Raji cells supported more expansion (41-fold) than one prior round of exposure to Raji cells (23-fold). Exposure to SKOV3 cells first, than Raji cells, resulted in less expansion, from 4-fold (1 round of exposure to SKOV3) to 2-fold (2 rounds of exposure to SKOV3). Again, the differences in increase in response to initial Raji cell stimulation versus CAR T cells alone or to initial SKOV3 stimulation were highly significant at days 8, 12 and 15 ($p < 0.001$, t-test for two independent samples for each comparison, using the raw data (n=3)). The graphed results are shown, normalized to maximum fold increase (Fig. 3a). The cells restimulated with SKOV3 first had not died, and they retained some cytotoxic activity, they simply did not expand as robustly as cells restimulated with Raji cells first.

The CAR-374 cells recovered from each round retained cytotoxic activity (Fig. 3b). In each cytotoxicity experiment the same number of CAR T cells were presented to luciferase-labeled target cells at a 5:1 E:T ratio. Representative results show that continual restimulation by Raji cells allows the CAR-374 T cell population to maintain very high cytotoxic activity against both JeKo-1 cells (a B lymphoma cell line) and SKOV3 cells (Fig. 3b). At both round 1 of cytotoxicity testing (after 1 stimulation) and round 3 of cytotoxicity testing (after 3 stimulations), cytotoxic activity was sufficient to kill >95% of the target cells. In contrast, continual restimulation by SKOV3 cells gradually impacted the ability of the CAR T cells to mediate full cytotoxic activity. After 1 stimulation, CAR-374 T cells were able to kill 100% of target tumor cells, whether JeKo-1 B cells or SKOV3 ovarian carcinoma cells (Fig. 3b). By round 3 of cytotoxicity testing, CAR T cells restimulated with SKOV3 cells partially lost cytotoxic potential

by approximately 80% (Fig. 3b). Similar results were seen with the control CAR-CD19 T cells (CAR-254) and the control CAR-Her2 T cells (CAR-390), whereby diminished cytotoxic capacity was only seen when T cells were restimulated by SKOV3 cells (Fig. 3c). The difference in cytotoxic activity of CAR-374 cells when stimulated with Raji cells versus SKOV3 cells was significant at Round 3 whether the target cell was JeKo-1 or SKOV3 ($p < 0.001$, t-test for two independent samples for each comparison, using the raw data (n=3)).

Bridging protein-secreting CAR-CD19 T cells are cytotoxic *in vivo*

Having established that CAR-142 T cells have cytotoxic activity against CD19-positive Nalm6 cells and Her2-positive SKOV3 cells *in vitro*, we tested the activity of these cells *in vivo*. We analyzed the circulating half-life of the purified bridging protein (#42) by injecting immunodeficient mice IV or i.p. with 100 μg of protein and analyzing protein concentration in the serum. The $T_{1/2}$ was determined to be 121 minutes after IV administration and 153 minutes after i.p. adminstration (Supplemental Fig. S4). The short half-life was expected given the small size of the bridging protein and the absence of any half-life extension technology such as an Fc-domain, a PEG-domain or an anti-albumin binding domain.

We tested the activity of the CAR-CD19, CAR-142 and CAR-374 T cells using xenografts in NOD-SCID-gamma common chain-deficient (NSG) mice. NSG mice injected iv with the CD19-positive leukemic cell line Nalm6 develop disseminated leukemia which is lethal three to five weeks after injection. CAR-CD19 T cells effectively eliminated the *in vivo* growth and dissemination of Nalm6 cells as expected (data not shown). To evaluate CAR-CD19 T cells secreting bridging proteins, we injected 1 x 10^6 Nalm6-luciferase cells on day 1 and allowed the leukemic cells to expand for 4 days. The baseline degree of luminescence was established, mice

were placed randomly into cohorts, and 3 different doses of CAR-T cells were injected iv. Mice were imaged weekly to determine the extent of disease burden. A dose response was observed for CAR-CD19 T cells (CAR-142 and CAR-374), with full eradication observed at the higher doses (Fig. 4a,b). This study demonstrates that CAR-CD19 T cells that secrete CD19-anti-Her2 bridging proteins (ie. CAR-142 and CAR-374) recognize and eliminate CD19-positive cells *in vivo.*

Figure 4. Her2-bridging CAR-CD19 T cells are efficacious *in vivo*. A) Dose responsive elimination of pre-established leukemia in an NSG mouse model was monitored after Her2-bridging CAR-CD19 T cells (CAR-142 and CAR-374) were administered at doses ranging from 2 x 10^6 to 1 x 10^7 cells/mouse. Luminescence values for all cohorts (A) and the treatment cohorts (B) are shown. C) CAR-142 T cells control SKOV3 tumor growth while control CAR T cells (CAR-254) have no effect. D) CAR-142 T cell control of SKOV3 tumor growth as compared to CAR-Her2 (CAR-390). CAR-142 and CAR-390 fully controlled tumor growth, while control mice succumbed and had to be euthanized by day 42 (panel E).

Next we extended the *in vivo* modeling to the Her2-positive tumor cell line SKOV3. SKOV3 cells (1 x 10^6) were implanted subcutaneously and allowed to establish and grow to a palpable size. Mice were then randomized, the baseline degree of luminescence was established, and 1 x 10^7 CAR T cells were injected iv on day 14, at which time the tumors averaged 150mm^3 by caliper measurement. CAR-CD19 T cells (CAR-254) and CAR-142 T cells were evaluated in this model. Mice were imaged weekly and caliper measurements of the tumor were taken twice weekly. By day 14 post CAR T cell injection the cohorts that received the CAR-142 T cells secreting the CD19-anti-Her2 bridging protein had cleared the tumor mass as measured by caliper (Fig. 4c). Indeed, the luminescent signature was the same as the background signature as determined using mice that had no tumor injection and no treatment (data not shown). Tumor growth was significantly less than that measured in the negative-control cohorts (CAR-CD19

injected mice, or untreated mice (NA), Fig. 4c). In a second study the *in vivo* activity of CAR-142 T cells and CAR-Her2 T cells (CAR-390, Table 1) was compared. The tumor control curves and the survival curves were indistinguishable (Fig. 4 d,e). All mice treated with CAR-142 or CAR-390 survived to day 42, while all animals in the negative control groups had to be sacrificed due to tumor burden. CAR-CD19 T cells secreting the stabilized CD19-Her2 bridging protein (CAR-374) performed similarly (Fig. 5a,b) except that there was the loss of one animal by the end of the study due to tumor burden (Fig. 5c).

Figure 5. Her2-bridging CAR-CD19 T cells eliminate Her2-positive tumors and CD19-positive tumors in a serial challenge *in vivo* model. A) CAR-374 treatment eliminated preestablished SKOV3 tumors in the NSG mouse model. B) 90% of CAR-374 treated mice survived past day 36, by which point the control mice were beginning to require euthanasia. C) CAR-374 that survived the SKOV3 challenge subsequently cleared CD19-positive Nalm6 leukemia challenge.

The mice treated with CAR-374 that had completely cleared the SKOV3 tumor were rested until day 55 (post tumor challenge) and then 4 mice were rechallenged with 1 x 10^6 Nalm6 cells to investigate whether the remaining CAR T cell pool could react to directly presented CD19 antigen. Three naïve NSG mice were also injected with 1 x 10^6 Nalm6 cells as a positive control for tumor engraftment and growth. The mice that had initially cleared the SKOV3 tumor effectively eliminated the Nalm6 cells, and there was no Nalm6 engraftment or expansion (Fig. 5d). In contrast the naïve mice challenged with Nalm6 cells rapidly developed disseminated leukemia (Fig. 5d) and were sacrificed by day 21 due to tumor burden.

These studies demonstrated that both mechanisms inherent to bridging-protein-secreting CAR-CD19 T cells were active *in vivo*: the T cells could eliminate CD19-positive Nalm6 cells

directly via the CAR-CD19 domain and also indirectly, via recognition of the CD19 ECD on the bridging protein that bound to the Her2-positive tumor cells.

Discussion

Here we describe a novel approach to CAR-T cell therapy with three unique attributes: first, we demonstrate that it is possible to retarget CAR-CD19 T cells to kill any solid or hematologic tumor cell, exemplified here using the Her2-positive solid tumor cells; second, we encode the CAR-CD19 domain and the CD19-bridging protein together within a lentiviral vector, such that it is secreted in parallel with expression of the CAR on the transduced T cell surface, thereby leveraging the inherent advantages of CAR-CD19 T cells; and third, we use modular CD19-bridging proteins, which apply well understood protein-engineering principles and solutions to multiple limitations facing the CAR-T cell field, including providing a platform for multi-antigen targeting.

Robust *in vivo* expansion followed by prolonged CAR-T cell persistence is critical for the efficacy of CAR-T cell therapy directed to the B cell tumor antigen CD19 for the treatment of hematological malignancies [26-28]. In contrast, most solid tumor-targeted CAR-T cells appear to have poor persistence properties, irrespective of the antigen targeted. For example, in a phase 1 clinical study of CAR T cell therapy for biliary tract and pancreatic cancers, Her2-targeting CAR-T cells showed peak expansion of 7-fold or less above baseline at day 9 post-injection, dropping thereafter [29]. Similarly, CAR-T cells targeting EGFRvIII that were administered for the treatment of glioblastoma persisted 21 days or less after infusion and had minimal clinical impact [30,31]. A CAR-T cell therapy targeting IL13Rα2 reported sustained clinical impact in one patient despite minimal CAR cell persistence, and there were no other notable responses in that trial [32]. Notably, CAR T cells targeting PSMA expanded up to 500-fold over baseline following administration of 10^9 – 10^{10} total T cells to patients [33]. Expansion in patients appeared to be Il-2-dependent and lasted up to 4 weeks; several partial clinical responses were noted, but the

duration of response was not reported. In general, poor CAR T persistence in solid tumors is associated with minimal clinical efficacy.

Advances in the field focused on improving CAR-T cell activity include providing cytokine or chemokine support, preventing immunosuppression, and targeting intrinsic pathways to improve CAR-T cell fitness and persistence [34-37]. Recent efforts to provide artificial and immunologically favorable antigen presentation to CAR T cells also aim to improve CAR T cell fitness and persistence. For example an exogenously added CAR-T ligand was developed that binds to albumin, traffics to lymph nodes and is displayed by antigen-presenting cells (APC) [38]. CAR-T cells that encounter this ligand in the lymph node are therefore stimulated not only by the displayed antigen but also by costimulatory receptors and cytokines produced by the APCs. In another example, *in vivo* administration of a nanoparticulate RNA vaccine was used to deliver a CAR antigen into lymphoid compartments in order to stimulate adoptively transferred CAR-T cells. Again, presentation of the target antigen on APCs promotes immunologically productive activation and expansion of the injected CAR-T cells [39]. Notably, engagement of relevant stimulatory, chemokine and adhesion signals appears to favor the development of T cell memory [40], a critical element in long term immune protection. Finally, the importance of immunologically relevant T cell activation has been demonstrated in the immune checkpoint field, with defined roles for organized secondary and tertiary lymphoid organs becoming apparent [41-44].

In our system the CAR-CD19 T cell interaction with normal B cells will support production of immunologically relevant stimulatory signals including adhesion interactions, chemokine and cytokine signals, and costimulatory signals [45-48]. This organic presentation of immunologically relevant antigen does not require administration of additional agents or

exogenous antigen, since B cells are APCs and represent a self-renewing source of CD19 that are present in lymphoid organs and in circulation. Moreover, in the *in vitro* experimental setting we showed that interaction of the Her-2 bridging CAR-CD19 T cells with a B cell target cell (Raji cells or Daudi cells) had a distinctly different outcome that interaction with a solid tumor cell target (SKOV3), suggesting that at least some T cell supportive signals are present even if the target B cell is malignant. In the *in vivo* model, serial presentation of antigens (Her2, CD19) showed that the Her2-bridging CAR-CD19 T cells could engage both cell types.

Even in the setting of B cell leukemias and lymphomas, expression of CD19 on normal B cells may be critical for prolonged persistence of CAR T cells. In fully murine (syngeneic) models of CAR-CD19 therapy of B cell malignancy, control of tumor cell outgrowth over time and in the context of leukemic rechallenge required the presence of normal B cells [49,50]. This observation suggests a unique role for normal B cells in providing a non-tumor dependent, self-renewing antigen source to support CAR-CD19 persistence. This concept is clinically validated, since some CAR-CD19-treated patients who have relapsed with CD19-negative tumors have persistent CAR-CD19 T cells in their circulation and continued B cell aplasia, demonstrating that the CAR-CD19 T cells remain functional [51]. An analysis of CAR-CD19 treatment of B cell leukemias found that the primary driver of CAR-CD19 T cell expansion and durable functional persistence was a cumulative burden of >15% of CD19 expressing leukemic and normal B cells in the bone marrow prior to lymphodepletion, and furthermore, that neither CAR T cell dose nor leukemia burden alone could predict CAR-CD19 T cell expansion and duration of engraftment [14,52]. These results strongly suggest a critical role for normal CD19-positive B cells is supporting CAR-CD19 T cell expansion and persistence. In the setting of CAR-CD19 T cells secreting

bridging proteins, CD19 expressed on normal B cells will be a readily accessed antigen source, to allow immunologically relevant CAR T cell expansion and to enhance persistence regardless of the targeted tumor antigen and indication.

The phenomena of tumor antigen loss in response to CAR-T cell therapy is observed across indications and antigens and represents another major issue confronting adoptive cell therapy. The findings to date include the loss of target antigens from the cell surface in hematologic malignancies including ALL, NHL and multiple myeloma, and rapid tumor cell population escape due to the heterogeneity of antigen expression in solid tumors [53-55]. It is clear that countering resistance due to antigen loss and tumor antigen heterogeneity will require multi-antigen targeting solutions. Our use of CD19-bridging proteins provides a simple and pragmatic solution to this problem since CD19-bridging proteins can be readily produced in single-antigen, dual-antigen and multi-antigen targeting formats. As shown herein, a bi-specific CD19-bridging protein containing an anti-Her2 and an anti-EGFR scFv killed tumor cell expressing one or the other antigen, while showing exceptional potency when both antigens were present. Likewise, the CD19-anti-CD20 bridging protein enables dual antigen targeting on B cell tumors using a single CAR-CD19 T cell. A CD19-bridging protein containing both anti-Clec12a and anti-CD33 VHH domains killed acute myeloid leukemia cells expressing either antigen. We have used VHH domains in many of our constructs, and the linkage of two, three or more VHHs in series is well-established [56]. Rapid flexible and modular extension to three or more antigens is readily achievable with the CD19-bridging protein format, which builds on decades of established antibody and antibody fragment-based solutions [56,57].

There are alternative elegant solutions to dual antigen targeting, including tandem CARs, dual CARs and gated CARs [58-60]; these are created via manipulation of the encoded CAR domain

sequence, which then must be successfully expressed on the T cell surface. As such technologies are extended to solid tumor antigens the expression of antigen on normal tissues will become a concern (see below), and may necessitate tuning of CAR affinities. Extension to three or more antigens while still retaining tumor targeting selectivity will require precise engineering. For example a recent paper described the use of defined ankyrin repeat domains (DARPins) to target three antigens successfully [61]. The technology was limited however as the potency of the trispecific CAR was lower than the corresponding monospecific CARs against tumor cells expressing a single target, revealing a potential limitation of multi-specific designs when expressed on the CAR T cell surface. Further, the issue of normal tissue cytotoxicity (eg. on EGFR) was not addressed. Thus the elegance of multi-CAR technologies is balanced by the difficulty, to date, of successfully engineering and expressing optimal constructs. In contrast, secretion or cell surface expression of proteins concurrent with CAR expression in CAR-CD19 T cells is well-established. This includes cytokines, receptors, and antibody domains, among others [35,62]. Further, BiTE protein secretion from activated T cells or CAR-T cells does not activate, anergize or exhaust the T cells despite the fact that these proteins bind back to T cells via their anti-CD3 component [63]. For example, an anti-CD3 x anti-EGFR BiTE was successfully secreted from an EGFRvIII-directed CAR-T cell showing that such secretion does not interfere with T cell function [8]. Further, both EGFR and EGFRvIII were specifically targeted in this system, demonstrating the utility of multi-antigen targeting from a single CAR T cell. In our system the secreted bridging protein likewise does not bind back to the CAR T cell in a manner that interferes with T cell function, and similarly enables multi-antigen targeting. The result is potent retargeted killing of the CD19-negative target cells with retention of cytotoxicity against CD19-positive cells.

Our approach offers additional advantages. As a discrete entity, the secreted bridging protein has no obvious liabilities. The half-life is very short, which will limit systemic exposure and binding to normal tissues via the antigen-binding domains. Further, there is no Fc-domain that might mediate immune activation. The CD19 ECD is also essentially inert, having low potential immunogenicity [18] and no detectable binding to target cells expressing CD21 and/or CD81 that normally function, in cis, to mediate CD19 signaling within the B cell receptor complex. Finally, no detectable CAR-CD19-dependent killing can be seen in the presence of CD19 ECD alone [18]. We conclude that as a discrete entity, a bridging protein is functionally inert and has limited systemic exposure. Thus secreted bridging proteins should be biased to accumulate only where cell and antigen density is most abundant, ie. in the tumor itself, and should therefore primarily mediate activation of a CAR-CD19 T cell when bridging to an antigen-positive tumor cell. Such a system should provide a superior therapeutic index when compared to antigen-targeting CAR T cells. One compelling translational strategy is to target Her2-positive CNS metastases in breast cancer, a leading cause of therapy failure. Systemically injected Her2-bridging CAR-CD19 T cells will expand in the presence of normal B cells, even if a patient remains on anti-Her2 antibody therapy. Activated CAR-CD19 T cells readily access the CNS where they can find and control cancers [64,65].

In summary, we present a universal method to retarget CAR-CD19 T cells to hematologic or solid tumor antigens, using CD19-bridging proteins secreted by the CAR-CD19 itself. This approach retains all the advantages of CAR-CD19 T cells, including optimal fitness and persistence and well a developed manufacturing history. In addition, the focus on protein engineering to create flexible and modular CD19-bridging proteins modulation provides simple solutions to potency, antigen selectivity, and multi-antigen targeting.

Materials and Methods

Human cell lines

SKOV3-luciferase (Cell Biolabs, San Diego, CA) were grown in RPMI containing 10% FBS and 0.8 mg/ml neomycin. BT474, Nalm6, K562, U937, Jeko-1, H929 and 293T cells (ATCC, Manassas, VA), Raji cells (MilliporeSigma, St. Louis, MO), and 293FT cells (Thermo Fisher, Waltham, MA) were cultured according to supplier specifications. Stable cell lines expressing firefly luciferase were generated using lentiviral particle transduction and puromycin selection (GeneCopoeia, Rockville, MD).

Protein expression constructs

Genes encoding wildtype CD19 extracellular domains (ECD) and scFvs were chemically synthesized by GenScript (Piscataway, NJ). The genes were assembled into pcDNA3.1+, pcDNA3.1+C-6HIS, or pcDNA3.1Hygro+ (Invitrogen, Carlsbad, CA). The CD19 ECD-A constructs contain the CD19 extracellular domain from amino acids 1 to 278, from UniProtKB accession number P15391. The CD19 ECD-B constructs contain a slightly longer CD19 extracellular domain, amino acids 1 to 291, from UniProtKB accession number P15391. Construct #28 contains the CD19 ECD-A plus a 6x His tag. For construct #42, a G4S linker sequence was placed between the CD19 ECD-A and the humanized anti-Her2 scFv (human 4D5 scFv, VH-G4Sx3-VL) derived from trastuzumab [66]. A 6x His tag was placed at the C terminus. Construct #117 contained the CD22 ECD amino acids 20-332 with a N101A mutation (UniProtKB accession number P20273), a G4S linker and the anti-Her2 scFv sequence with a His tag. For construct #311, the wildtype CD19 sequence of construct #42 was replaced with an N terminal stabilized CD19 mutant of CD19 ECD-B [18]. Construct #340 is identical to #311, but

uses stabilized CD19 ECD-A. Construct #416 contains stabilized CD19 ECD-B, a G4S linker and an anti-EGFR scFv sequence derived from panitumumab VH and VL sequences (Genbank accession numbers LY588610 and LY588596, respectively) and contains a 6x His tag. Construct #460 contains the trastuzumab scFv, a G4S linker, the C terminal stabilized CD19 ECD-A, a second G4S linker, the panitumumab anti-EGFR scFv and a 6x His tag. It was produced by ligation of the pantitumumab fragment into a vector containing the trastuzumab-CD19 fusion.

Expression of the bridging proteins

293T cells were transfected with expression constructs using lipofectamine 2000 following the manufacturer's protocol (Invitrogen, Waltham, MA). On day 3 post transfection the cell culture supernatants were harvested via centrifugation at 12,000 RPM for 4 minutes at 4ºC. His tagged bridging proteins were purified from the 293T transfected cell supernatant using a Ni Sepharose HisTrap excel column following the manufacturer's protocol (GE Healthcare, Marlborough, MA). The relevant fractions were pooled and buffer exchanged to PBS.

Gel filtration

Cell culture media was initially run on a Ni-sepharose column and the bound protein was eluted and analyzed by PAGE and Western blot (Lake Pharma, Belmont, CA). Fractions containing protein were run over a Superdex200 column to separate monomeric from oligomeric protein (Lake Pharma, Belmont, CA).

CAR-T cell generation

For production and characterization of CAR T cells, CD3-positive human primary T cells were isolated from PBMC derived from normal human donors (Research Blood Components, Watertown, MA) and cultivated in ImmunoCult-XF T cell expansion medium (serum/xeno-free) supplemented with 50 IU/ml IL-2 at a density of 3 x 10^6 cells/mL, activated with CD3/CD28 T

cell Activator reagent (STEMCELL Technologies, Vancouver, Canada) and transduced on day 1 with the CAR lentiviral particles in the presence of 1X Transdux (Systems Biosciences, Palo Alto, CA). Cells were propagated until harvest on day 10. Post-expansion, CAR T cells were stained with FLAG antibody to measure CAR expression. Briefly, 1 x 10^5 cells were incubated with anti-FLAG antibody (Thermo Fisher), diluted 1:100 in PBS for 60 minutes at 10°C, followed by a 1:100 dilution of anti-rabbit APC-conjugated antibody (Thermo Fisher). CAR T cells were stained for CD8 using anti-CD8 MEM-31 antibody, diluted 1:100 (Thermo Fisher). Cells were resuspended in PBS and fixed at a final concentration of 2% paraformaldehyde. Cell populations were analyzed using an Accuri C6 flow cytometer (BD Biosciences, Franklin Lakes, NJ).

Lentivirus production

For the production of lentiviral particles, packaging plasmids pALD-VSVG-A, pALD-GagPol-A and pALD-Rev-A (Aldevron, Fargo, ND) and the expression plasmid were combined in Opti-MEM (Invitrogen). Trans-IT transfection reagent (Mirus, Madison, WI) was added. After incubation, the DNA/Trans-IT mixture was added to 293FT cells in Opti-MEM. After 24 hours, the media replaced with DMEM plus 10% FBS daily for 3 days and stored at 4°C. The viral particles were precipitated by adding 5X PEG-IT (Systems Biosciences) incubating at 4°C for 72 hours. The mixture was centrifuged at 3000 RCF for 30 minutes, the residual supernatant removed and the pellet resuspended in 200 µl PBS and stored at -80°C.

CAR constructs

Construct #254 sequence contains the FMC63 anti-CD19 CAR. The anti-CD19 scFv sequence was derived from the FMC63 antibody [67], cloned in the VL-VH orientation, and

includes a FLAG-tag, CD28 linker, transmembrane domain and cytoplasmic signaling domain (amino acids 114-220, UniProtKB accession number P10747) plus 4-1BB (amino acids 214-255, UniProtKB accession number Q07011) and CD3ς (amino acids 52-164, UniProtKB accession number P20963) cytoplasmic signaling domains. The sequence was chemically synthesized (GenScript) and cloned into a derivative of the lentiviral vector, pCDH-CMV-MCS-EF1-Neo (Systems Biosciences) that contains an MSCV promoter. Construct #390 is a CAR-Her2 containing an scFv (Vh-Vl) from the anti-Her2 antibody FRP5 (GenBank accession number A22469) followed by the same components as the CAR-254 (Flag tag, CD28 stalk transmembrane and cytoplasmic signaling domain and the 4-1BB and CD3ς cytoplasmic signaling domains). The scFv portion of the CAR was chemically synthesized (Integrated DNA Technologies, Coralville, IA) and then assembled with a PCR fragment from the CAR-254 vector, minus the anti-CD19 scFv, using the NEBuilder Hi Fi DNA Assembly Master Mix (New England Biolabs, Beverly, MA).

CAR-CD19 constructs containing bridging proteins

The inserts for the following vectors, #142, #374, #174, #373, #173 and #221 were chemically synthesized (Lentigen Technology, Gaithersburg, MD) and cloned into their lentivirus vector containing an MSCV promoter. All contain the CAR-CD19 sequence described for CAR-254, a P2A cleavage site, and a bridging protein sequence containing a wildtype or stabilized form of CD19. Construct #142 contains the wildtype CD19 ECD plus the trastuzumab scFv-His bridging protein as described for #42. Construct #374 contains the bridging protein #340 (stabilized CD19-G4S linker-trastuzumab scFv). Construct #174 contains the wildtype CD19-ECD-anti-CD20 leu16 scFv-His bridging protein. The anti-CD20 leu16 VH-VL scFv sequence

was slightly modified from the published sequence [68]. Construct #373 is similar to #174 but it contains the anti-CD20 leu16 scFv followed by the CD19 ECD with C terminal stabilizing mutations [18]. Construct #173 contains a bridging protein with the wildtype CD19 ECD and an anti-BCMA scFv (Vh-Vl from US 2016/0297885, SEQ ID No. 357 and 358). Construct #221 contains a bridging protein with wildtype CD19 ECD and an anti-Clec12a scFv (derived from Genbank Accession number ADR89994).

Protein Analysis

Purified proteins were loaded at 0.1 μg protein per lane for western blot analysis and 8 μg protein per lane for coomassie blue gel staining, and were separated by electrophoresis on NuPAGE 4-12% Bis-Tris gels (Invitrogen) run at a constant 100 volts. The gel was stained with 25% ethanol, 10% acetic acid, 0.2 g/L Coomassie Brilliant Blue G-250 (Sigma, St. Louis, MO) and destained with 5% acetic acid, 10% ethanol. For western blot analysis the gel was transferred using iBlot 2 NC Mini Stacks the iBlot2 instrument (Invitrogen). The membrane was blocked in TBST (0.1 M Tris, pH7.4, 0.5 M NaCl, 0.5% Tween20) with 5% non-fat dry milk for 1 hour and followed by adding 1:1000 dilution of HRP-anti-His antibody (BioLegend, Dedham, MA) in TBST with 1% non-fat dry milk for additional 3 hours. The blot was developed with SuperSignal Western Femto Maximum Sensitivity Substrate (Thermo Fisher) and the image was detected with the Chemi Doc MP Imaging system (BioRad, Hercules, CA).

Analysis of bridging protein binding, specificity and affinity by ELISA

Plates were coated overnight at 4°C with 1.0 μg/mL anti-CD19 antibody FMC63 (#NBP2-52716, Novus Biologics, Centennial, CO) or 1.0 μg/mL purified Her2-Fc (#HE2-

H5253, AcroBiosytems, Newark, DE), in 0.1 M carbonate, pH 9.5. The plate was blocked with 0.3% non-fat milk in TBS for 1 hour at room temperature. After washing in TBST 3 times, the bridging protein was titrated from a starting concentration of 5 µg/mL using serial 3-fold dilutions in TBS/1% BSA and incubated 1 hour at room temperature. Detection with Her2-Fc, biotinylated Her2 (#He2-H822R, AcroBiosystems), or antibody FMC63 was performed by adding the detection reagent at 1.0 µg/mL and incubating for 1 hour at room temperature. The plates were then washed 3 times, followed by a 1 hour incubation with a 1:2000 dilution of anti-human IgG-HRP (#109-035-088, Jackson ImmunoResearch, West Grove, PA) for Her2-Fc detection, HRP-steptavidin (#21130, Thermo Fisher) for biotinylated Her2 detection, and anti-mouse IgG-HRP (#115-035-062, Jackson ImmunoResearch) for FMC63 detection. Then, 1-Step Ultra TMB-ELISA solution (#34028, Thermo Fisher) was added to develop the peroxidase signal, and the plate was read at 405 nm. Curves were fit using a four parameter logistic regression to calculate the EC_{50}.

Flow cytometric analyses of bridging protein binding to cells and of cell surface antigen expression

When necessary, cells to be analyzed were detached with 0.5 mM EDTA in PBS. Tumor cells or lymphocytes were washed and analyzed in ice cold FACS buffer (PBS/1 % BSA/0.1% sodium azide). Cells were resuspended (5 x 10^5/100 µl) and purified bridging proteins (up to 10 µg/ml), or supernatants (100 µl) were added to 100 µl final volume and incubated with the cells at 4°C for 30 minutes. After washing, cells were resuspended (5 x 10^5/100 µl) and incubated with detection antibody at 4°C for 30 minutes. The cells were resuspended in 100 µl total volume and stained with 5 µl anti-His-PE (#IC050P, R&D Systems, Minneapolis, MN) or anti-CD19

antibody FMC63-PE (#MAB1794, MilliporeSigma, Burlington, MA) for 30 minutes at 4ºC , washed and resuspended using PBS, fixed with 1% paraformadehyde in PBS, and analyzed on the Accuri Flow Cytometer (BD Biosciences). Analysis of antigen expression by tumor cells was performed using PE-conjugated monoclonal antibodies specific for the target antigen. Analysis of T cell antigen expression was performed using PE-conjugated or APC-conjugated monoclonal antibodies specific for the target antigen.

Analysis of secreted bridging protein concentration by ELISA

To measure the secretion of bridging protein by CAR T cells, 600,000 cells were added at $3x10^6$ cells/ml to a 96-well U-bottom plate. Cells were activated with 1X ImmunoCult Human CD3/CD28 T Cell Activator (#10971, Stemcell Technologies) and cultured for 4 days. The cells were briefly centrifuged at 300 x g for 4 minutes and the supernatants were collected. The amount of bridging protein was measured in an ELISA assay. For the ELISA, a 96 well plate was coated with 1.0 µg/ml anti-CD19 antibody FMC63 (#NBP2-52716, Novus Biologics) in 0.1 M carbonate, pH 9.5 overnight at 4°C. The plate was blocked with 0.3% non-fat milk in TBS for 1 hour at room temperature (RT). After washing the plate 3 times in TBST (0.1 M Tris, 0.5 M NaCl, 0.05% Tween20), 100 µl of culture supernatant was added and incubated for 1 hour at room temperature. Purified #42 protein was used to generate the ELISA standard curve. The plate was washed 3 more times in TBST and HRP-anti-His (BioLegend) was added at a 1:2000 dilution at room temperature for 1 hour in the dark. To develop the peroxidase enzymatic signal, 1-Step Ultra TMB-ELISA solution (Thermo Fisher) was added and the plate read was at 405 nm on a plate reader. The standard curves were generated using a four parameter logistic (4PL) and used to calculate the concentration of the unkown.

Cytotoxicity assays

Target tumor cell lines were stably transfected with a luciferase cDNA. Cells were seeded at $1x10^4$/25 µl cells per well in a 96 well round (suspension) or opaque flat (adherent) bottom plate in RPMI 1640 containing 10% FBS, without antibiotics. When included, dilutions of bridging proteins were made in 100 µl media and added to the cells. CAR T cells were thawed, washed once with media and recovered via centrifugation at 550 x g for 10 minutes at 4ºC. CAR T cells were added to the wells containing target cells to give an effector:target cell ratio of 10:1, 5:1, 3:1, 2:1, 1:1, as desired, in a volume of 25 µl. In experiments using the standard CAR-CD19 T cells, bridging proteins were added as noted. The plates were incubated at 37ºC for 48 hours. For suspension cells, the plate was centrifuged at 550 x g for 5 minutes at room temperature, the pellet was rinsed with PBS, spun again, then lysed with 20 µl 1x lysis buffer (Promega). The lysate was transferred into a 96 well opaque tissue culture plate (Thermo Fisher). For adherent cell lines, the cell culture supernatant was removed, the cells were washed twice with cold PBS and then the 1x lysis buffer was added to the well. The plates were read in a luminometer having an injector (Glomax Multi Detection System, Promega, Madison, WI). The percent killing was calculated based upon the average loss of luminescence of the experimental condition relative to the control wells containing only target cells.

Order of addition assay

Target tumor cell lines Nalm6 and SKOV3 cells were seeded at 1 x 10^4 cells per well in 50 µl in a 96 well round bottom plate for Nalm6 and 96 well white opaque plate for SKOV in RPMI 1640 containing 10% FBS without antibiotics. The bridging proteins #42 or #340 were applied at final concentration of 1 µg/ml in 25 µl media per well. CAR-254 T cells (58% Flag+) were thawed, washed once with media and recovered via centrifugation at 550 x g for 10 minutes at 4ºC. The CAR T cells were applied to the well at a 10:1 ratio to the target cells in 25 µl

volume. Three conditions were applied as following: (1) the target cell, the bridging protein and the CAR T cells were added simultaneously, (2) the target protein and the bridging protein were preincubated at 37°C for 10 minutes then the CAR T cells were added, (3) the bridging protein and CAR T cells were preincubated at 37°C for 10 minutes then added to the target cells. The plates were incubated at 37°C for 48 hours. Nalm6 target cells in round bottom plates were centrifuged at 550 x g for 5 minutes at 4°C, and the cell pellet was rinsed with PBS. SKOV3 target cells in white opaque plates were directly rinsed with PBS. The cells were lysed with 20 µl 1x lysis buffer (#E1501, Promega). The lysate was transferred into a 96 well opaque tissue culture plate. The plates were read in a luminometer having an injector (Glomax Multi Detection System, Promega). The percent killing was calculated based upon the average loss of luminescence of the experimental condition relative to the control wells containing only target cells (ie. no cytotoxicity). Positive controls were CAR-254 (for Nalm6 cytotoxicity) and CAR-390 (for SKOV3 cytotoxicity).

Restimulation assay

On day 0, the CAR T and target cell cultures were set up at 2:1 (CD3+ CAR T: target cells at $2x10^4$: $1x10^4$ cells/well), and incubated for 96 hours. For the re-stimulation step, the CD3+ T cell number/well information was obtained from anti-CD3-APC staining (#300411, BioLegend) and beads count according to the manufacturer's protocol (#580, Bangs Laboratories, Inc. Fishers, IN). The CAR T cells were stimulated every 4 days with mitomycin C (MMC) treated Raji or SKOV3 cells. The cells were treated with 5 mg/ml MMC (#BP2531-2, Fisher Scientific) for 90 minutes at 37°C and then washed twice with RPMI medium before adding to the T cells at a 2:1 ratio (CAR T:MMC treated cells). Before each restimulation, 100 µl

of media was removed and 100 µl of MMC treated Raji or SKOV3 cells in fresh media were added on days 4, 8 and 12. Prior to each restimulation, parallel killing assays were set up on Day 0 (R0 = fresh out of frozen), Day 4 (Round 1), Day 8 (Round 2), Day 12 (Round 3) and Day 15 (Round 4). The CAR T cells were counted, pooled spun at 500 x g for 10 minutes and then resuspended at $5x10^5$ cells/ml. The cytotoxicity assay was set up as described above on JeKo-1 and SKOV3 cells at a 5:1 E:T ratio.

In vivo modeling

The half-life of the wildtype CD19 ECD-anti-Her2 scFv bridging protein #42 was determined using SCID mice (n=10) injected IV or IP with 5 µg/kg of protein. The half-life of the stabilized CD19 ECD-anti-Her2 scFv-anti-albumin sdAb-His bridging protein #432 was determined using by ELISA assay. Blood samples were taken just prior to injection and at 30 minutes, 90 minutes, 6 hours, 24 hours, 48 hours, 72 hours, 96 hours and 120 hours. Whole blood was collected via the tail vein (100 µL per bleed). Whole blood was collected into EDTA K3 tubes (#411504105, Sarstedt, Numbrecht, Germany). The blood samples were spun for 10 minutes at 8500 rpm. The plasma was then transferred to a 1.5ml eppendorf tubes and frozen until analysis by ELISA. A 96 well plate (Pierce, 15041) was coated with 1.0 µg/ml FMC63 (Novus, NBP2-52716) in 0.1 M carbonate, pH 9.5 overnight at 4°C. The plate was blocked with 0.3% non-fat milk in TBS for 1 hour at room temperature. After washing in TBST (0.1 M Tris, 0.5 M NaCl, 0.05% Tween20) 3 times, the fusion protein in the serum was 3-fold diluted in 1% BSA in TBS and add 50 µl per well. Purified #42 (prepared by Lake Pharma, Hopkinton, MA) was used to create the standard starting curve, with 1 µg/ml with serial 3x titration. The plate was incubated for 1 hour at room temperature. The plate was washed 3 times in TBST, and HRP-anti-His antibody (#652504, BioLegend) was added at a 1:2000 dilution. The plate was incubated at

room temperature in the dark for 1 hour. Then, 1-Step Ultra TMB-ELISA solution (#34028, Thermo Fisher) was added to the plate, and the plate was read at 405 nm. The standard curves were fit using a four parameter logistic (4PL) regression to calculate the protein concentration in the unknown serum samples.

Animal efficacy models were performed under an institutional IACUC protocol (Cummings School of Veterinary Medicine at Tufts University, Grafton, MA). NOD/Scid x common-gamma chain-deficient (NSG) mice were purchased (Jackson Laboratories, Bar Harbor, ME) and allowed to acclimate in cage details for at least 3 days after receipt. For all studies the following criteria were used to monitor animal health and allow for humane euthanasia as needed. Lethargy, poor coat condition, poor body condition, abnormal ambulation, and weight loss (>10%) were general health parameters used to determine a euthanasia endpoint. In addition, in the subcutaneous solid tumor studies, mice were euthanized if the tumor mass reached 1500mm^3. Any animals reaching any endpoint criterion were euthanized on the same day. No animals died prior to meeting the criteria for euthanasia.

To establish a systemic leukemia model, NSG mice were injected IV with 1 x 10^6 Nalm6-luciferase cells on day one. Luciferase activity was monitored by the injection of luciferin (150mg/kg) followed by immediate whole animal imaging. Leukemia cells were allowed to engraft and expand for 4 days. The baseline degree of luminescence was established by imaging (IVIS 200, Perkin Elmer, Waltham, MA), and mice were randomized into experimental cohorts. There were 10 mice per cohort (n=10) unless otherwise indicated. Mice were injected with CAR T cells on day 4 and imaged weekly to determine the extent of disease burden. Animals were sacrificed when tumor burden or animal health indicated, per the IACUC protocol.

To establish a solid tumor model we implanted 1 x 10^6 SKOV3-luciferase cells subcutaneously in the flank and allowed the tumors to grow to a palpable size of ~150mm^3 on average. Mice were then randomized and CAR T cells were injected IV the following day. There were 10 mice per cohort (n=10) unless otherwise indicated. Caliper measurements of tumor volume were taken 2x weekly. Animals were sacrificed when tumor burden or animal health indicated, per the IACUC protocol.

References

1. O'Leary MC, Lu X, Huang Y, et al: FDA Approval Summary: Tisagenlecleucel for Treatment of Patients with Relapsed or Refractory B-cell Precursor Acute Lymphoblastic Leukemia. Clin Cancer Res 25:1142-1146, 2019

2. Bouchkouj N, Kasamon YL, de Claro RA, et al: FDA Approval Summary: Axicabtagene Ciloleucel for Relapsed or Refractory Large B-cell Lymphoma. Clin Cancer Res 25:1702-1708, 2019

3. Dai X, Mei Y, Cai D, et al: Standardizing CAR-T therapy: Getting it scaled up. Biotechnol Adv 37:239-245, 2019

4. Alabanza L, Pegues M, Geldres C, et al: Function of Novel Anti-CD19 Chimeric Antigen Receptors with Human Variable Regions Is Affected by Hinge and Transmembrane Domains. Mol Ther 25:2452-2465, 2017

5. Qin H, Ramakrishna S, Nguyen S, et al: Preclinical Development of Bivalent Chimeric Antigen Receptors Targeting Both CD19 and CD22. Mol Ther Oncolytics 11:127-137, 2018

6. Schneider D, Xiong Y, Wu D, et al: A tandem CD19/CD20 CAR lentiviral vector drives on-target and off-target antigen modulation in leukemia cell lines. J Immunother Cancer 5:42, 2017

7. Chmielewski M, Abken H: TRUCKs: the fourth generation of CARs. Expert Opin Biol Ther 15:1145-54, 2015

8. Choi BD, Yu X, Castano AP, et al: CAR-T cells secreting BiTEs circumvent antigen escape without detectable toxicity. Nat Biotechnol 37:1049-1058, 2019

9. Neelapu SS: Managing the toxicities of CAR T-cell therapy. Hematol Oncol 37 Suppl 1:48-52, 2019

10. Ying Z, Huang XF, Xiang X, et al: A safe and potent anti-CD19 CAR T cell therapy. Nat Med 25:947-953, 2019

11. Duong MT, Collinson-Pautz MR, Morschl E, et al: Two-Dimensional Regulation of CAR-T Cell Therapy with Orthogonal Switches. Mol Ther Oncolytics 12:124-137, 2019

12. Mestermann K, Giavridis T, Weber J, et al: The tyrosine kinase inhibitor dasatinib acts as a pharmacologic on/off switch for CAR T cells. Sci Transl Med 11, 2019

13. Park JH, Geyer MB, Brentjens RJ: CD19-targeted CAR T-cell therapeutics for hematologic malignancies: interpreting clinical outcomes to date. Blood 127:3312-20, 2016

14. Finney OC, Brakke HM, Rawlings-Rhea S, et al: CD19 CAR T cell product and disease attributes predict leukemia remission durability. J Clin Invest 129:2123-2132, 2019

15. Forsberg MH, Das A, Saha K, et al: The potential of CAR T therapy for relapsed or refractory pediatric and young adult B-cell ALL. Ther Clin Risk Manag 14:1573-1584, 2018

16. Lee DW, Kochenderfer JN, Stetler-Stevenson M, et al: T cells expressing CD19 chimeric antigen receptors for acute lymphoblastic leukaemia in children and young adults: a phase 1 dose-escalation trial. Lancet 385:517-528, 2015

17. Knochelmann HM, Smith AS, Dwyer CJ, et al: CAR T Cells in Solid Tumors: Blueprints for Building Effective Therapies. Front Immunol 9:1740, 2018

18. Klesmith JR, Su L, Wu L, et al: Retargeting CD19 Chimeric Antigen Receptor T Cells via Engineered CD19-Fusion Proteins. Mol Pharm 16:3544-3558, 2019

19. De Oliveira SN, Wang J, Ryan C, et al: A CD19/Fc fusion protein for detection of anti-CD19 chimeric antigen receptors. J Transl Med 11:23, 2013

20. Ajina A, Maher J: Strategies to Address Chimeric Antigen Receptor Tonic Signaling. Mol Cancer Ther 17:1795-1815, 2018

21. Tedder TF, Zhou LJ, Engel P: The CD19/CD21 signal transduction complex of B lymphocytes. Immunol Today 15:437-42, 1994

22. Sato S, Miller AS, Howard MC, et al: Regulation of B lymphocyte development and activation by the CD19/CD21/CD81/Leu 13 complex requires the cytoplasmic domain of CD19. J Immunol 159:3278-87, 1997

23. Wang D, Starr R, Alizadeh D, et al: In Vitro Tumor Cell Rechallenge For Predictive Evaluation of Chimeric Antigen Receptor T Cell Antitumor Function. J Vis Exp, 2019

24. Garcia-Cozar FJ, Molina IJ, Cuadrado MJ, et al: Defective B7 expression on antigen-presenting cells underlying T cell activation abnormalities in systemic lupus erythematosus (SLE) patients. Clin Exp Immunol 104:72-9, 1996

25. Petru E, Sevin BU, Perras J, et al: Comparative chemosensitivity profiles in four human ovarian carcinoma cell lines measuring ATP bioluminescence. Gynecol Oncol 38:155-60, 1990

26. Porter DL, Hwang WT, Frey NV, et al: Chimeric antigen receptor T cells persist and induce sustained remissions in relapsed refractory chronic lymphocytic leukemia. Sci Transl Med 7:303ra139, 2015

27. Fraietta JA, Lacey SF, Orlando EJ, et al: Determinants of response and resistance to CD19 chimeric antigen receptor (CAR) T cell therapy of chronic lymphocytic leukemia. Nat Med 24:563-571, 2018

28. Schultz L, Mackall C: Driving CAR T cell translation forward. Sci Transl Med 11, 2019

29. Feng K, Liu Y, Guo Y, et al: Phase I study of chimeric antigen receptor modified T cells in treating HER2-positive advanced biliary tract cancers and pancreatic cancers. Protein Cell 9:838-847, 2018

30. Johnson LA, Scholler J, Ohkuri T, et al: Rational development and characterization of humanized anti-EGFR variant III chimeric antigen receptor T cells for glioblastoma. Sci Transl Med 7:275ra22, 2015

31. O'Rourke DM, Nasrallah MP, Desai A, et al: A single dose of peripherally infused EGFRvIII-directed CAR T cells mediates antigen loss and induces adaptive resistance in patients with recurrent glioblastoma. Sci Transl Med 9, 2017

32. Brown CE, Alizadeh D, Starr R, et al: Regression of Glioblastoma after Chimeric Antigen Receptor T-Cell Therapy. N Engl J Med 375:2561-9, 2016

33. Junghans RP, Ma Q, Rathore R, et al: Phase I Trial of Anti-PSMA Designer CAR-T Cells in Prostate Cancer: Possible Role for Interacting Interleukin 2-T Cell Pharmacodynamics as a Determinant of Clinical Response. Prostate 76:1257-70, 2016

34. Castellarin M, Watanabe K, June CH, et al: Driving cars to the clinic for solid tumors. Gene Ther 25:165-175, 2018

35. Mardiana S, Solomon BJ, Darcy PK, et al: Supercharging adoptive T cell therapy to overcome solid tumor-induced immunosuppression. Sci Transl Med 11, 2019

36. Lynn RC, Weber EW, Sotillo E, et al: c-Jun overexpression in CAR T cells induces exhaustion resistance. Nature 576:293-300, 2019

37. Stampouloglou E, Cheng N, Federico A, et al: Yap suppresses T-cell function and infiltration in the tumor microenvironment. PLoS Biol 18:e3000591, 2020

38. Ma L, Dichwalkar T, Chang JYH, et al: Enhanced CAR-T cell activity against solid tumors by vaccine boosting through the chimeric receptor. Science 365:162-168, 2019

39. Reinhard K, Rengstl B, Oehm P, et al: An RNA vaccine drives expansion and efficacy of claudin-CAR-T cells against solid tumors. Science, 2020

40. Mayya V, Judokusumo E, Abu-Shah E, et al: Cutting Edge: Synapse Propensity of Human Memory CD8 T Cells Confers Competitive Advantage over Naive Counterparts. J Immunol 203:601-606, 2019

41. Cabrita R, Lauss M, Sanna A, et al: Tertiary lymphoid structures improve immunotherapy and survival in melanoma. Nature, 2020

42. Petitprez F, de Reynies A, Keung EZ, et al: B cells are associated with survival and immunotherapy response in sarcoma. Nature, 2020

43. Helmink BA, Reddy SM, Gao J, et al: B cells and tertiary lymphoid structures promote immunotherapy response. Nature, 2020

44. Knoblich K, Cruz Migoni S, Siew SM, et al: The human lymph node microenvironment unilaterally regulates T-cell activation and differentiation. PLoS Biol 16:e2005046, 2018

45. Dustin ML: Role of adhesion molecules in activation signaling in T lymphocytes. J Clin Immunol 21:258-63, 2001

46. Commins SP, Borish L, Steinke JW: Immunologic messenger molecules: cytokines, interferons, and chemokines. J Allergy Clin Immunol 125:S53-72, 2010

47. Fooksman DR, Vardhana S, Vasiliver-Shamis G, et al: Functional anatomy of T cell activation and synapse formation. Annu Rev Immunol 28:79-105, 2010

48. Greenwald RJ, Freeman GJ, Sharpe AH: The B7 family revisited. Annu Rev Immunol 23:515-48, 2005

49. Yang Y, Kohler, M.E., Fry, T.J.: Effect of chronic endogenous antigen restimulation on CAR T cell persistence and memory formation. Blood 130:166, 2017

50. Cheadle EJ, Hawkins RE, Batha H, et al: Natural expression of the CD19 antigen impacts the long-term engraftment but not antitumor activity of CD19-specific engineered T cells. J Immunol 184:1885-96, 2010

51. DiNofia AM, Maude SL: Chimeric Antigen Receptor T-Cell Therapy Clinical Results in Pediatric and Young Adult B-ALL. Hemasphere 3:e279, 2019

52. Singh N, Frey NV, Grupp SA, et al: CAR T Cell Therapy in Acute Lymphoblastic Leukemia and Potential for Chronic Lymphocytic Leukemia. Curr Treat Options Oncol 17:28, 2016

53. Majzner RG, Mackall CL: Tumor Antigen Escape from CAR T-cell Therapy. Cancer Discov 8:1219-1226, 2018

54. Timmers M, Roex G, Wang Y, et al: Chimeric Antigen Receptor-Modified T Cell Therapy in Multiple Myeloma: Beyond B Cell Maturation Antigen. Front Immunol 10:1613, 2019

55. Akhavan D, Alizadeh D, Wang D, et al: CAR T cells for brain tumors: Lessons learned and road ahead. Immunol Rev 290:60-84, 2019

56. Bannas P, Hambach J, Koch-Nolte F: Nanobodies and Nanobody-Based Human Heavy Chain Antibodies As Antitumor Therapeutics. Front Immunol 8:1603, 2017

57. Gonzalez-Sapienza G, Rossotti MA, Tabares-da Rosa S: Single-Domain Antibodies As Versatile Affinity Reagents for Analytical and Diagnostic Applications. Front Immunol 8:977, 2017

58. Roybal KT, Rupp LJ, Morsut L, et al: Precision Tumor Recognition by T Cells With Combinatorial Antigen-Sensing Circuits. Cell 164:770-9, 2016

59. Grada Z, Hegde M, Byrd T, et al: TanCAR: A Novel Bispecific Chimeric Antigen Receptor for Cancer Immunotherapy. Mol Ther Nucleic Acids 2:e105, 2013

60. Tu S, Zhou X, Guo Z, et al: CD19 and CD70 Dual-Target Chimeric Antigen Receptor T-Cell Therapy for the Treatment of Relapsed and Refractory Primary Central Nervous System Diffuse Large B-Cell Lymphoma. Front Oncol 9:1350, 2019

61. Balakrishnan A, Rajan A, Salter AI, et al: Multispecific Targeting with Synthetic Ankyrin Repeat Motif Chimeric Antigen Receptors. Clin Cancer Res 25:7506-7516, 2019

62. Guedan S, Calderon H, Posey AD, Jr., et al: Engineering and Design of Chimeric Antigen Receptors. Mol Ther Methods Clin Dev 12:145-156, 2019

63. Ellerman D: Bispecific T-cell engagers: Towards understanding variables influencing the in vitro potency and tumor selectivity and their modulation to enhance their efficacy and safety. Methods 154:102-117, 2019

64. Frigault MJ, Dietrich J, Martinez-Lage M, et al: Tisagenlecleucel CAR T-cell therapy in secondary CNS lymphoma. Blood 134:860-866, 2019

65. He X, Xiao X, Li Q, et al: Anti-CD19 CAR-T as a feasible and safe treatment against central nervous system leukemia after intrathecal chemotherapy in adults with relapsed or refractory B-ALL. Leukemia 33:2102-2104, 2019

66. Carter P, Presta L, Gorman CM, et al: Humanization of an anti-p185HER2 antibody for human cancer therapy. Proc Natl Acad Sci U S A 89:4285-9, 1992

67. Nicholson IC, Lenton KA, Little DJ, et al: Construction and characterisation of a functional CD19 specific single chain Fv fragment for immunotherapy of B lineage leukaemia and lymphoma. Mol Immunol 34:1157-65, 1997

68. Wu AM, Tan GJ, Sherman MA, et al: Multimerization of a chimeric anti-CD20 single-chain Fv-Fc fusion protein is mediated through variable domain exchange. Protein Eng 14:1025-33, 2001

Figure 1.

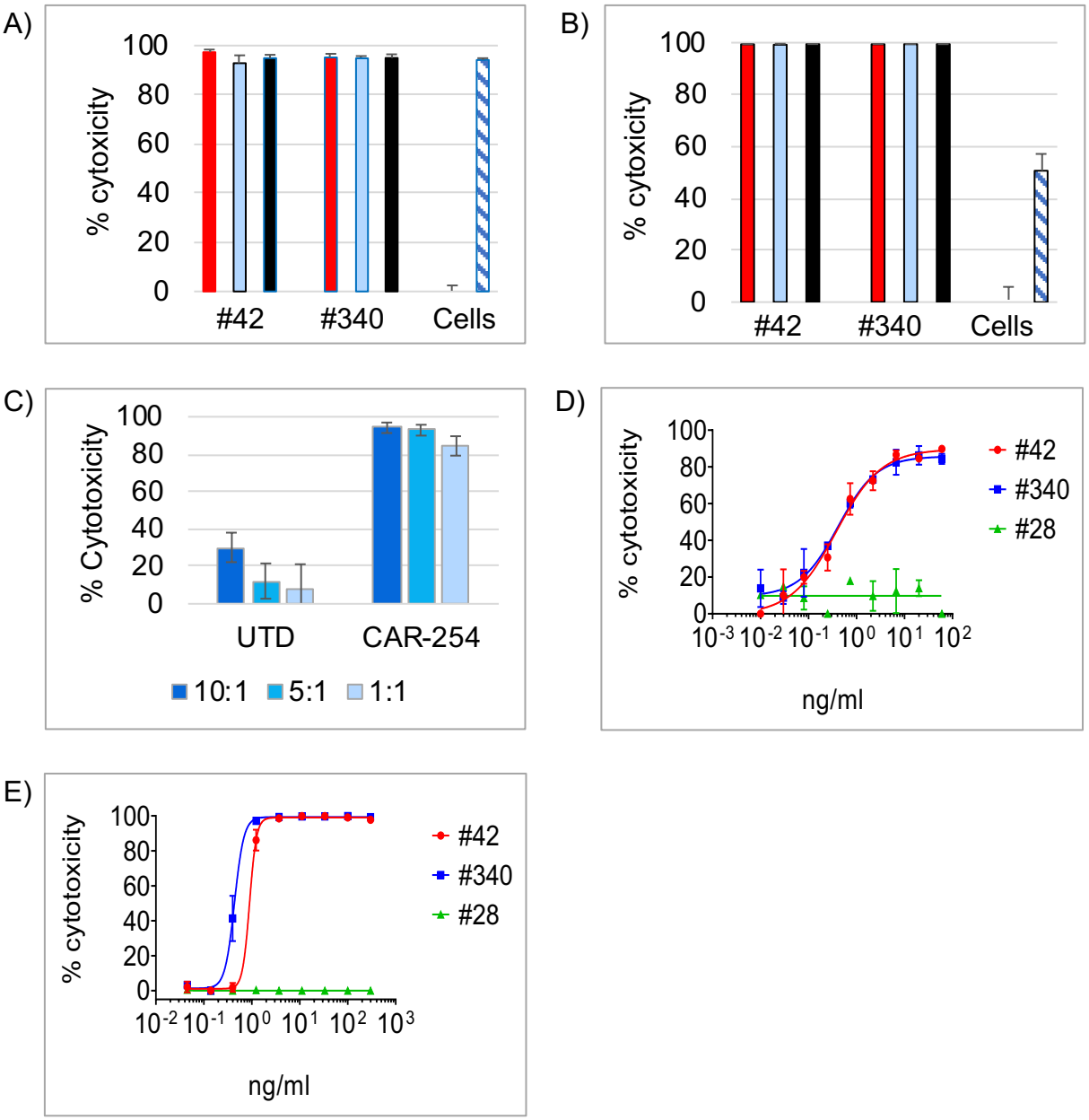
A)
% cytoxicity
100
80
60
40
20
0
#42
#340
Cells
B)
% cytoxicity
100
80
60
40
20
0
#42
#340
Cells
C)
% Cytotoxicity
100
80
60
40
20
0
UTD
CAR-254
10:1
5:1
1:1
D)
% cytotoxicity
100
80
60
40
20
0
10-3 10-2 10-1 100 101 102
ng/ml
#42
#340
#28
E)
% cytotoxicity
100
80
60
40
20
0
10-2 10-1 100 101 102 103
ng/ml
#42
#340
#28

Figure 2.

A)

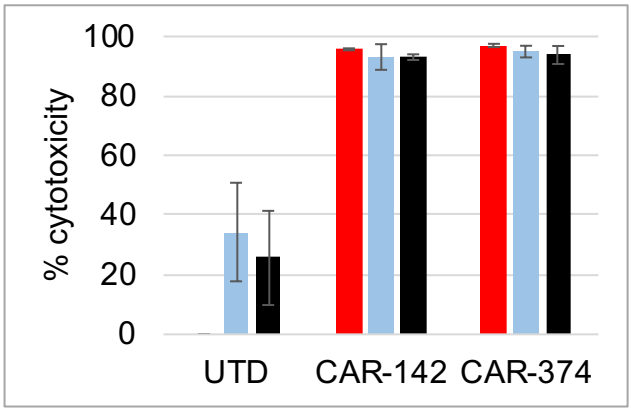
100
80
60
40
20
0
% cytotoxicity
UTD
CAR-142
CAR-374

B)

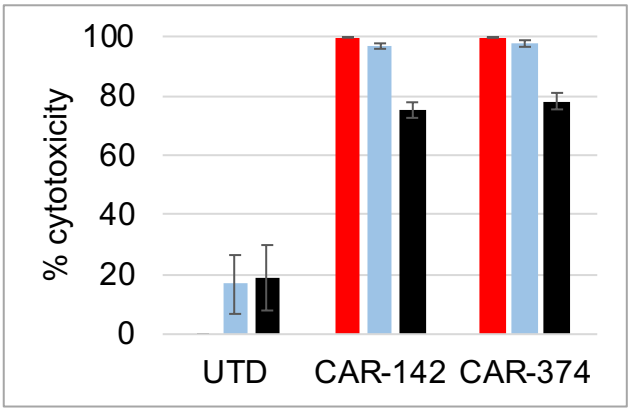
100
80
60
40
20
0
% cytotoxicity
UTD
CAR-142
CAR-374

Figure 3.

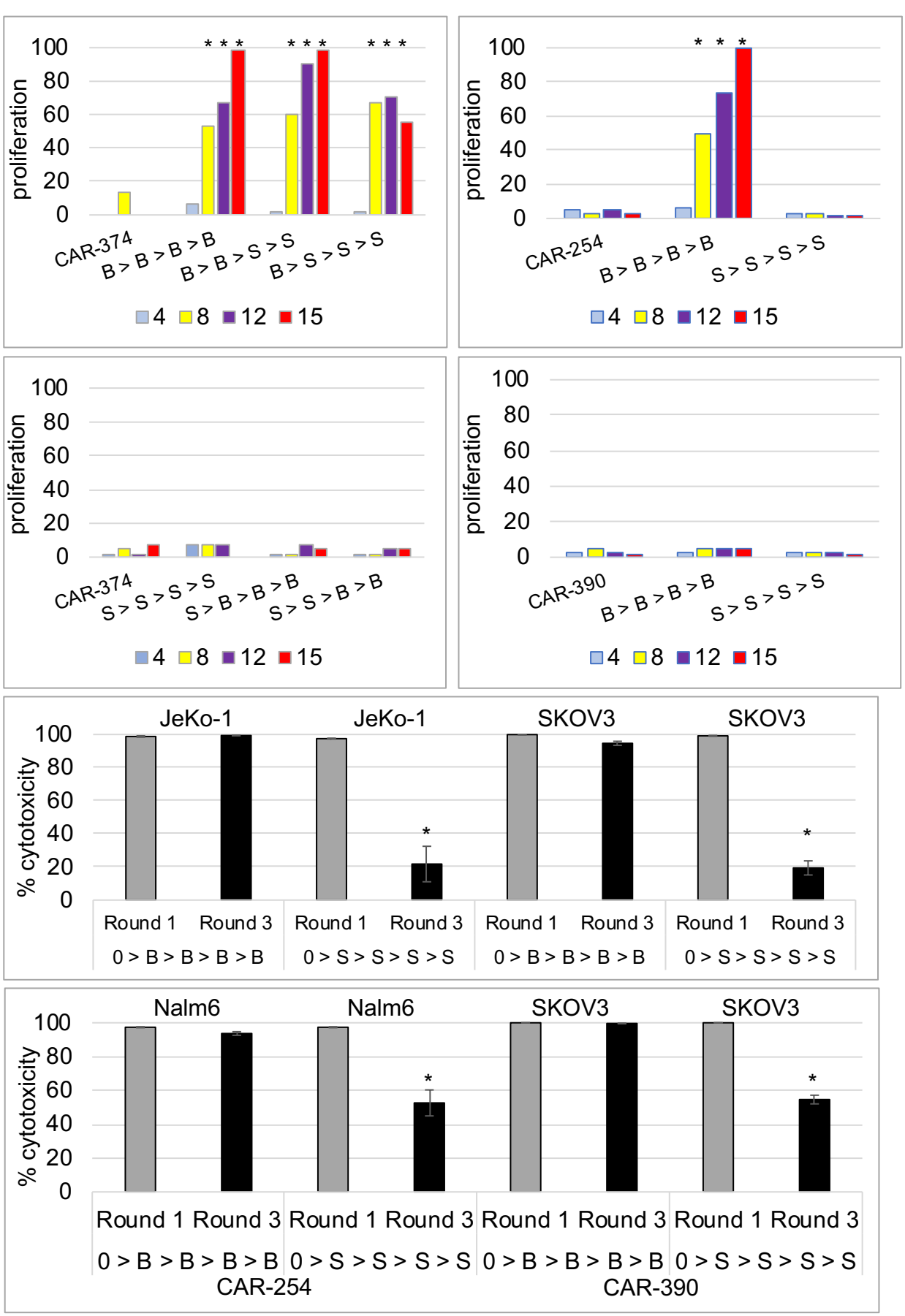
A)
proliferation
100
80
60
40
20
0
CAR-374
B > B > B > B
B > B > S > S
B > S > S > S
CAR-254
S > S > S > S
CAR-390
4 8 12 15
B)
% cytotoxicity
JeKo-1
JeKo-1
SKOV3
SKOV3
Round 1 Round 3
0 > B > B > B > B
0 > S > S > S > S
C)
Nalm6
Nalm6
SKOV3
SKOV3
CAR-254
CAR-390

Figure 5.

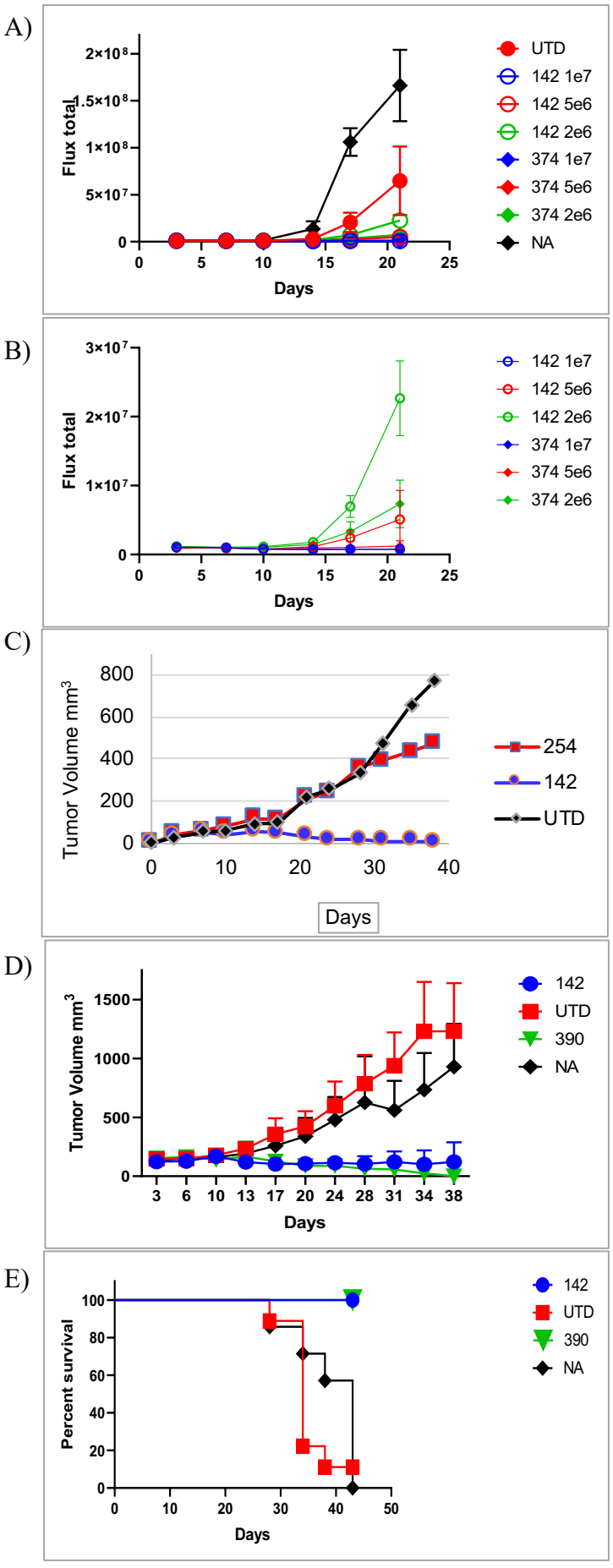
A)
Flux total
2×10⁸
1.5×10⁸
1×10⁸
5×10⁷
0
0 5 10 15 20 25
Days
UTD
142 1e7
142 5e6
142 2e6
374 1e7
374 5e6
374 2e6
NA
B)
Flux total
3×10⁷
2×10⁷
1×10⁷
0
0 5 10 15 20 25
Days
142 1e7
142 5e6
142 2e6
374 1e7
374 5e6
374 2e6
C)
Tumor Volume mm³
800
600
400
200
0
0 10 20 30 40
Days
254
142
UTD
D)
Tumor Volume mm³
1500
1000
500
0
3 6 10 13 17 20 24 28 31 34 38
Days
142
UTD
390
NA
E)
Percent survival
100
80
60
40
20
0
0 10 20 30 40 50
Days
142
UTD
390
NA

Figure 5.

A)

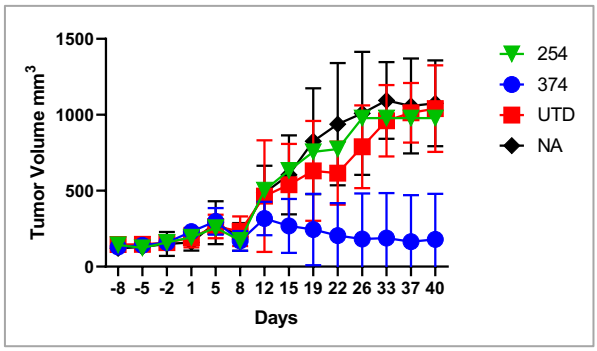
Tumor Volume mm3
1500
1000
500
0
-8 -5 -2 1 5 8 12 15 19 22 26 33 37 40
Days
254
374
UTD
NA

B)

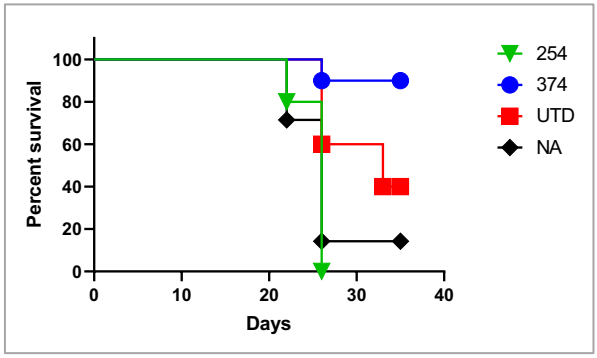
Percent survival
100
80
60
40
20
0
0 10 20 30 40
Days
254
374
UTD
NA

C)

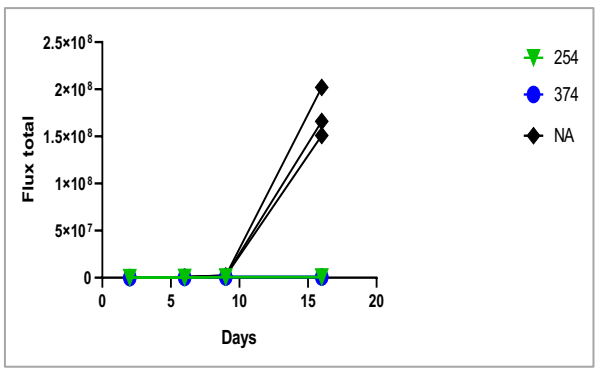
Flux total
2.5×10^8
2×10^8
1.5×10^8
1×10^8
5×10^7
0
0 5 10 15 20
Days
254
374
NA